Non-Linear Control of Quasi-Z-Source Inverter with Battery for Renewable energy Systems Based on Interconnection-Damping-Assignment Passivity-Based Control

Gholam Reza Shahabadi[1], Majid Reza Naseh[2*], Siavash Es'haghi[3]

Abstract-Due to the growing popularity of renewable energy sources, grid-connected inverters are becoming more and more common in distributed microgrid and smart-grid system. The appropriate characteristics of Quasi-Z-source inverters (QZSI), including continuous input current, common DC rail, and high voltage gain, have made these inverters widely used in the renewable energy system. A battery is necessary for renewable energy systems in order to store energy when the demand for power is low. IN this study a configuration involving a battery across one of the capacitors on the DC side is proposed, through which the DC control loop is adjusted. Also, Interconnection-Damping-Assignment Passivity-Based Control (IDA-PBC)approach has been used to adjust the battery current/voltage and the output voltage. Compared to other controllers, the proposed controller can provide faster response and better stability for QZSI when the variation of input and load. In addition, the proposed controller is not sensitive to the system's initial operating point and is global asymptotic stability. The simulations and theoretical design show the effectiveness of the proposed controller.

1. Introduction

Z-source inverters(ZSI) are a new-generation inverter topologies that have been widely used in various applications. The basic ZSI topology was first proposed by F. Z. Peng [1]. QZSI are a modified version of ZSI that offers improved benefits and features[2]. QZSI inherently has all the advantages of ZSI. The advantages of QZSI in comparison with ZSI are continuous input current, common DC rail, high voltage gain, and reduction of stress of passive components[3].In light of the traits mentioned, QZSI topology is a highly attractive option for renewable energy purposes. This inverter has been used in applications such as photovoltaics, wind power, fuel cells, electric drives, and hybrid vehicle[4]. In new renewable energy systems, a battery is considered for energy storage. This battery is designed to store energy during times when the demand for power is low and the voltage level is satisfactory. The voltage stored within the battery is used during the period of the short supply voltage. Most articles focus on the design of QZSI with fewer components, higher efficiency, higher gain voltage and reliability[5-7]. In[8] controllers on the DC and AC side, is designed separately. In [9]the structure of ZSI with a battery has been utilized for electric vehicle systems. In [10] the structure of the QZSI with battery has been used in order to utilize the energy of the fuel cell. The topic of controlling the charging current for the QZSI with a battery is rarely brought up. The output voltage and charge current of the battery inside the QZSI system with the battery have to be managed by the shoot-through state, which complicates the control. Until regulate the DC side voltage, various control strategies, such as sliding mode control and PI control have been studied[11, 12]. Therefore, the proposed controllers are not applicable due to the integrity of the system under study. The QZSI possessing a battery is a system with a fifth-order nonlinearity. Therefore, it is necessary to design a non-linear controller that is robust to uncertainties.

In this study, IDA-PBC approach was used to control the output voltage and the battery current and voltage considered in the configuration. The dynamic performance of the system is analyzed for the different changes within the system, including input voltage, battery current and voltage, and AC load. The simulation result verify the

1 Department of Electrical Engineering, University of Applied Science and Technology, Tehran, Iran. Email:ghr.shahabady@gmail.com

2* Corresponding Author: Department of Electrical engineering, Birjand Branch, Islamic Azad University,Birjand, Iran. Email:naseh@iaubir.ac.ir

3Department of Electrical engineering, Birjand Branch, Islamic Azad University, Birjand, Iran Email: s_esshaghi@sbu.ac.ir

efficacy of the proposed control. This paper is organized as follows. The averaged state-space model of QZSI with battery is introduced in Section 2. In Section 3, PCH and IDA-PBC for the QZSI with battery have been investigated. Section 4 presents the simulation results and examines their implications. Finally, the conclusion is proposed in section 5.

2. Averaged state-space model of QZSI with battery

The system configuration of QZSI with battery is presented in Figure1. The QZSI consists of inductors (L_1, L_2), capacitors (C_1, C_2), a variable input voltage source (V_{in}) and a diode. The battery is connected across C_1. In this system, the battery charge current and DC voltage are regulated using a shoot-through. The modulation index control input is used to control the injection current into the grid. The performance of QZSI is as follows. QZSI operates in two modes for a defined range of input voltages. One is a non shoot–through state, and the other is a shoot-through state. In this configuration, all of the capacitors and inductors are considered ideal. The inverter section of the proposed topology is modeled by a current source and a switch.

2.1 non shoot-through state

During the non shoot–through state interval, the inverter will continue to function properly and only one of the two switches in the inverter leg will be active at a time. Therefore, the single switch is OFF and the QZSI equivalent circuit is shown in Figure 2. The KVL and KCL equations in this circuit are as follows:
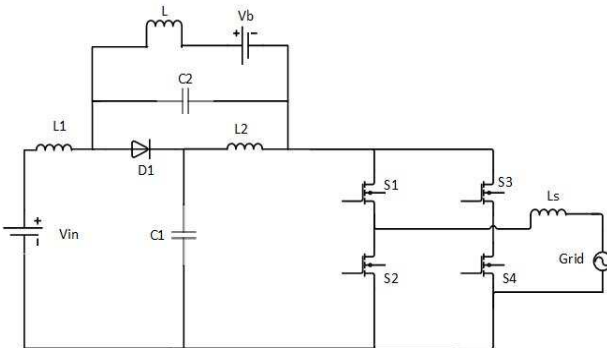
Fig. 1. Configuration of QZSI with battery for energy storage

$$\begin{cases} v_{L_1} = -v_{C_1} + v_{in}, v_{L_2} = -v_{C_2} \\ i_{C_1} = i_{L_1} - i_o, i_{C_2} = i_{L_2} - i_b - i_o \\ v_L = v_{C_2} - v_b \end{cases} \quad (1)$$
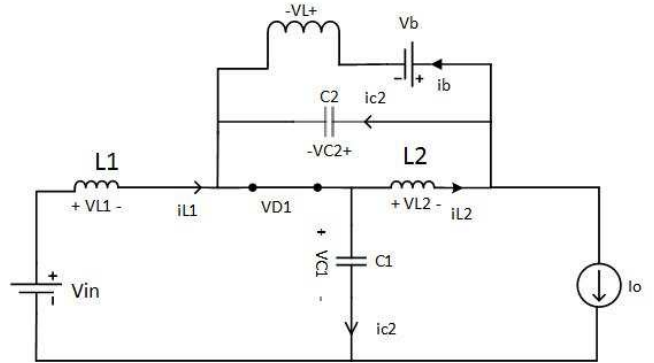
Fig. 2. Equivalent circuit in non-shoot through state

2.2 shoot-through state

During the shoot-through state interval, both switches of a leg are activated at the same time, causing the output of the impedance network to be short-circuited and the diode to be reversed. Hence, the single switch is activated and the QZSI equivalent circuit can be seen in Figure 3. The KVL and KCL equations in this circuit are as follows:

$$\begin{cases} v_{L_1} = v_{C_2} + v_{in}, v_{L_2} = v_{C_1} \\ i_{C_1} = -i_{L_2}, i_{C_2} = -i_{L_1} - i_b \\ v_L = v_{C_2} - v_b \end{cases} \quad (2)$$

2.3 The state-space averaged model

Using Eqs. (1) and (2), it is possible to derive the system state-space equation.
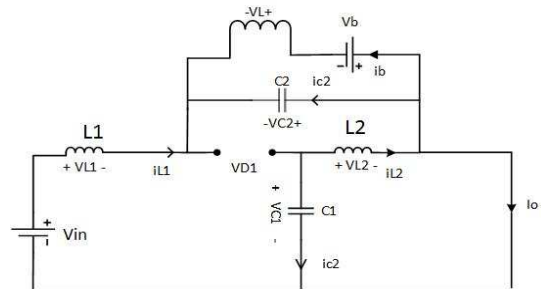
$$\dot{X} = A + Bu \quad (3)$$

Fig. 3. Equivalent circuit in shoot through state

Where:

$$A = \begin{bmatrix} \frac{1}{L_1}(-v_{C_1} + v_{in}) \\ \frac{-v_{C_2}}{L_2} \\ \frac{1}{C_1}(i_{L_1} - i_o) \\ \frac{1}{C_2}(i_{L_2} - i_b - i_o) \\ \frac{1}{L}(v_{C_2} - v_b) \end{bmatrix}, B = \begin{bmatrix} \frac{1}{L_1}(v_{C_1} + v_{C_2}) \\ \frac{1}{L_2}(v_{C_1} + v_{C_2}) \\ \frac{1}{C_1}(i_o - i_{L1} - i_{L_2}) \\ \frac{1}{C_2}(i_o - i_{L1} - i_{L_2}) \\ 0 \end{bmatrix} \quad (4)$$

The state vector includes five parameters as capacitor voltage v_{C_1} and v_{C_2}, inductor currents i_{L1} and i_{L_2}, and the battery charge/discharge current i_b. The state vector is:

$$X = \begin{bmatrix} i_{L_1} & i_{L_2} & v_{C_1} & v_{C_2} & i_b \end{bmatrix}^T \quad (5)$$

In (3), u is the shoot-though ratio, and i_o is the AC load current.

3. Port Controlled Hamiltonian System (PCHS)

In this section, we will model the QZSI provided by PCHS. Dynamic systems with energy storage elements can be described by the theory of PCHS as Eq. (6):

$$\dot{X} = [J(x) - R(x)]\frac{\partial H(x)}{\partial x} + g(x)u + \xi$$

$$y = g^T(x)\nabla H(x) \quad (6)$$

Which u, x and y are the control, state, and output variables of the system, respectively. y and u are called port variables and the product of these two variables shows the power injected into the system. In Eq.(6) $H(x): R^n \to R$ is energy function and is $(H(0) = 0, x \neq 0\ H(x) > 0)$.

Also $J(x) \in R^{n \times n}$ an interconnection matrice and $R(x) \in R^{n \times n}$ is the damping or dissipation matrice. The following relationships must be established for these matrices:

$$J(x) = -J^T(x)$$
$$R(x) = R^T(x) \geq 0 \quad (7)$$

$g \in R^{n \times m}$ demonstrates the kernel of the systems input matrice. It is widely accepted that stability in a system

relies heavily on its passivity."A system is called passive if the supply energy to the system is at least equal or more than the energy stored in that system for a particular time interval"[13].Mathematically this property is shown in Eq. (8):

$$\frac{dH(x)}{dt} = (\frac{\delta H(x)}{\delta x})^T \dot{x} =$$
$$-(\frac{\delta H(x)}{\delta x})^T R(x)(\frac{\delta H(x)}{\delta x}) + u^T y \leq u^T y \quad (8)$$

The basic and important characteristic of PCHS systems is the inherent inactivity and its stability. The Inequality (8) indicate that the energy stored in a passive system is always less than or equal to energy externally supplied to it, or in other words, a passive system is unable to generate energy [13].The energy balance equation (9) can be used to demonstrate the rate of change of total energy, as indicated in equation (8), by integrating the expression.

$$\underbrace{H[x(t) - H[x(0)]}_{Stored} = \underbrace{\int_0^t u^T(s)y(s)ds}_{Supplied} -$$
$$\underbrace{\int_0^t (\frac{\partial H[x(s)]}{\partial x})^T R[x(s)](\frac{\partial H[x(s)]}{\delta x})ds}_{dissipated} \quad (9)$$

It can be deduced from Eq. (9) that the energy stored in the system will always decrease due to dissipation until it reaches its lowest possible value[14]. The goal of control in these systems is to keep the system running close to the desired performance level.

3.1 PCHS modelling

In order to design a passivity-based controller, it is necessary to convert the system state space model to the form shown in Eq. (6). For this purpose, it is necessary to adapt matrices J, R and g by comparing Eqs. (4) and (6).

$$J(x) = \begin{bmatrix} 0 & 0 & \dfrac{-1}{L_1 C_1} & 0 & 0 \\[2mm] 0 & 0 & 0 & \dfrac{-1}{L_2 C_2} & 0 \\[2mm] \dfrac{1}{L_1 C_1} & 0 & 0 & 0 & 0 \\[2mm] 0 & \dfrac{1}{L_2 C_2} & 0 & 0 & \dfrac{-1}{L C_2} \\[2mm] 0 & 0 & 0 & \dfrac{1}{L C_2} & 0 \end{bmatrix}$$

$$R(x) = 0 \in R^{5 \times 5},$$

$$g(x) = \begin{bmatrix} \dfrac{x_3 + x_4}{L_1} \\[2mm] \dfrac{x_3 + x_4}{L_2} \\[2mm] \dfrac{i_o - x_1 - x_2}{C_1} \\[2mm] \dfrac{i_o - x_1 - x_2}{C_2} \\[2mm] 0 \end{bmatrix}, \xi = \begin{bmatrix} \dfrac{v_{in}}{L} \\[2mm] 0 \\[2mm] \dfrac{-i_o}{C_1} \\[2mm] \dfrac{-i_o}{C_2} \\[2mm] \dfrac{-v_b}{L} \end{bmatrix} \qquad (10)$$

3.2 IDA-PBC theory

As Eq.(6) indicates, in systems shown by Hamiltonian theory, the energy exchange of the system is performed using J and R matrices. The purpose of the IDA-PBC is to devote a desired energy function with a desired equilibrium point x_d by modifying the interconnection matrix $J_d(x)$, damping matrix $R_d(x)$ and control law [13].The resulting closed-loop system is shown in (16):

$$\dot{x} = [J_d(x) - R_d(x)] \frac{\partial H_d(x)}{\partial x} \qquad (11)$$

Which:

$$\begin{aligned} J_d(x) &= [J(x) + J_a(x)] = -J_d^T(x), \\ R_d(x) &= [R(x) + R_a(x)] = R_d^T(x) \geq 0, \qquad (12) \\ H_d(x) &= [H(x) + H_a(x)] \geq 0 \end{aligned}$$

Matrices and Functions the d subtitle is the desired matrices and functions. The new energy function denoted by $H_d(x)$ as a minimum point in $\tilde{x}$ ($H(\tilde{x}) = \arg\min H_d(x)$) such that $\tilde{x} \in R^n$. The desired balance point where the system needs to be stabilized is $\tilde{x}$.In this method of designing, a new energy function, interconnection matrix, and damping are all established. The open loop energy

function of the system is transformed into a close loop energy function based on Eq. (12). $H_a(x)$, $J_a(x)$ and $R_a(x)$ are designed such that:

$$J_a(x) = -J_a^T(x) \qquad (13)$$

$$R_a(x) = R_a^T(x) \qquad (14)$$

$$H_a(x) = H_a^T(x) \qquad (15)$$

that $J_a(x)$ and $R_a(x)$ are matrices that are both additively skew-symmetric and additively positive definite symmetric, respectively. To reach the desired dissipative and interconnection matrices for close loop system can $J_a(x)$ and $R_a(x)$ are designed based on Eq. (12). From Eq. (6) and (10), the following expression is derived.

$$\begin{aligned} [J(x) - R(x)] &\frac{\partial H(x)}{\partial x} + g(x)u + \xi = \\ & [J_d(x) - R_d(x)] \frac{\partial H_d(x)}{\partial x} \end{aligned} \qquad (16)$$

Therefore, substituting Eq. (12) into Eq. (16) yields:

$$(J - R)\nabla H_a = -(J_a - R_a)\nabla H_d + g(x)u + \xi \quad (17)$$

By selecting the appropriate J_a and R_a matrices, the control input can be calculated as the Eq. (18):

$$\begin{aligned} u(x) = g^+ [\{J_a(x) - R_a(x)\} &\frac{\partial H_d(x)}{\partial x} + \\ \{J(x) - R(x)\} &\frac{\partial H_a(x)}{\partial x}] \end{aligned} \qquad (18)$$

Where:

$$g^+ = \{g^T(x).g(x)\}^{-1} g^T(x) \qquad (19)$$

3.3 Controller design based on IDA-PBC

In this section, we select the interconnection and damping matrices in order to achieve the control objectives. Let $x_{id} (i = 1,2,3,4,5)$ denote the desired equilibrium states of the close-loop system. The desired close loop energy function is defined as:

$$\begin{aligned} H_d(x) = &\frac{1}{2} L_1 (x_1 - X_{1d})^2 + \frac{1}{2} L_2 (x_2 - X_{2d})^2 + \\ &\frac{1}{2} C_1 (x_3 - X_{3d})^2 + \frac{1}{2} C_2 (x_4 - X_{4d})^2 + \qquad (20) \\ &\frac{1}{2} L (x_5 - X_{5d})^2 \end{aligned}$$

The values of battery current and capacitor voltage that are parallel to the battery are selected as desired. By setting Eq. (4) to zero, the other values are selected as follows:

$$X_{5d} = I_{bref}$$
$$X_{4d} = V_{bref}$$
$$X_{3d} = V_{in} + V_{bref} \qquad (21)$$
$$X_{2d} = \frac{(V_{in} + V_{bref})I_o + V_{bref}I_{bref}}{V_{in}} + I_{bref}$$
$$X_{1d} = \frac{(V_{in} + V_{bref})I_o + V_{bref}I_{bref}}{V_{in}}$$

One solution is to choose the interconnection and damping matrices as (22):

$$J_a = 0 \in R^{5\times 5}$$
$$R_a = diag[r_1 \ r_2 \ r_3 \ r_4 \ r_5] \qquad (22)$$

Therefore, the damping and interconnection desired matrices can be defined as:

$$R_d = diag[r_1, r_2, r_3, r_4, r_5] \qquad (23)$$

$$J_d = J_a \qquad (24)$$

By specifying the desired connection and damping mat rices, the control input can be determined using (18).

3.4 Proof of stability

To validate the proposed control technique, the derivative of the suggested Hamiltonian function must be negative. The derivative of the function is calculated and shown in (25).

$$\dot{H}_d = (\nabla H_d(x))^T \dot{x} = \{\nabla H_d(x)\}^T$$
$$\{J_d(x) - R_d(x)\}\{\nabla H_d(x)\} \qquad (25)$$

As $J_d(x)$ possess a skew symmetric property in PCH form, it may be manifested that:

$$\{\nabla H_d(x)\}^T J_d(x)\{\nabla H_d(x)\} = 0 \qquad (26)$$

In addition, $R_d(x)$ is appositive definite matrice so:

$$\dot{H}_d(x) = -\{\nabla H_d(x)\}^T R_d(x)\{\nabla H_d(x)\} < 0 \quad (26)$$

Therefore, according to Eq. (26), the asymptotic stability of the system can be proved.

4. Results and discussion

This section provides simulations and their results to analyze the transient and steady state responses of the suggested controllers. Inverter and controller parameters are considered according to Table 1. The parameters used in Table 1 are selected based on the values in[11]. All of the simulations were performed using the MATLAB/Simulink toolbox (2018 version). Battery current and capacitor voltage that are parallel to the battery are considered as outputs.

Table 1. Nominal specifications of the QZSI with battery

Description	Symbol	Value
Input voltage	v_{in}	$100v - 200v$
Reference current of battery	I_{bref}	$10A$
DC-side inductors	$L_1 = L_2$	$400\mu H$
DC-side capacitors	$C_1 = C_2$	$500\mu F$
Inductance	L	$40\mu H$
Steady-state voltage of battery	v_b	$20v - 28v$

4.1 Steady-state response

Considering the parameters of the QZSI with battery in Table1, the steady-state response of the IDA-PBC is illustrated in Figure. 4. The reference voltage and current of the battery are respectively 20 V and 10 A. Also, the nominal value of the output current is considered to be 10 A.As shown in Figure. 4, the designed controller has a zero steady-state error in tracking the battery reference current and voltage. In Figure. (c) and (d) of Figure. 4, the values 20% higher and lower than the battery voltage and current are displayed in green. As seen in Figure. 4, within a short period of time, the voltage and current of the battery remain within a range of 20% of their permanent value. The control indicators for this situation are presented in Table 2.

4.2 The step-change of input voltage

In this case, QZSI is started with the battery in nominal condition. It is assumed that step changes in input voltage are applied from 100 to 300v. According to the results presented in Figure. 5, it can be seen that the controller response is stable and has a steady-state error of zero in tracking the battery reference current and voltage. It is also stable when changing input and has an acceptable transient response. In Figure. (c) and (d) of Figure. 5, the values 20% higher and lower than the battery voltage and current are displayed in green. As seen in Figure. 5, within a short period of time, the voltage and current of the battery remain within a range of 20% of their permanent value. The control indicators for this situation are presented in Table 2

4.3 The step-change of reference current of battery

In this test, the stability and robustness of the designed QZSI with the battery during the change of the reference current of the battery are investigated. The reference current of battery value is changed from 10 to 12 A at t =1s, which is more than a 20% variation around the operating point. According to the results presented in Figure. 6, it can be seen that the controller response is stable, and has a zero steady-state error in tracking the battery reference current. In addition, it is stable during the changing reference current of the battery and has an acceptable transient response. In Figure (c) and (d) of Figure6, the values 20% higher and lower than the battery voltage and current are displayed in green. The control indicators for this situation are presented in Table 2.

4.4 The step-change of reference voltage of battery

In addition, to study the stability and robustness of the developed IDA-PBC reference voltage of the battery is stepped from 20 to 28v at t = 3s. The Figure 7 shows that the controller designed for altering the reference voltage of the battery produces a consistent and satisfactory transient response. In Figurer(c) and (d) of Figurer 7, the values 20% higher and lower than the battery voltage and current are displayed in green. As seen in Figurer 7, within a short period of time, the voltage and current of the battery remain within a range of 20% of their permanent value. The control indicators for this situation are presented in Table 2.
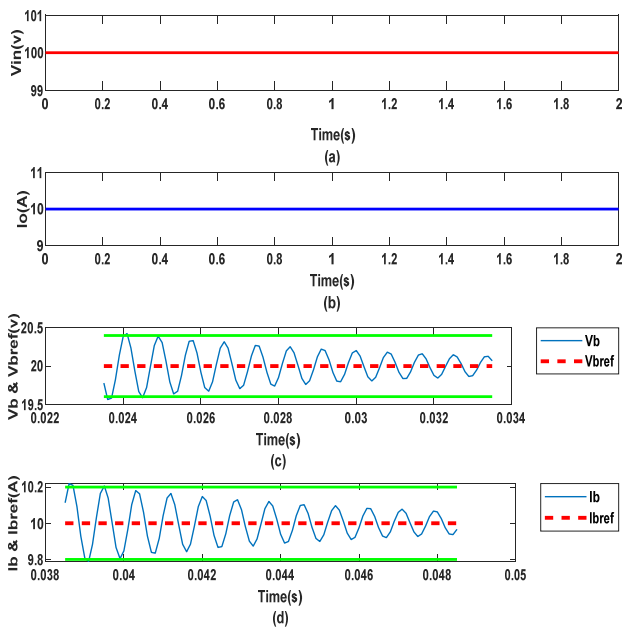
In this test, the stability of the QZSI designed with the battery when changing the load current is investigated. The nominal value of the output current changes from 10 to 15 A at t = 1s. The graph in Figure 8 shows that the controller is stable, and after a brief period, the current and voltage of the battery reach their desired values. In Figure (c) and (d) of Figure 8, the values 20% higher and lower than the battery voltage and current are displayed in green. As seen in Figure 8, within a short period of time, the voltage and current of the battery remain within a range of 20% of their permanent value. The control indicators for this situation are presented in Table 2.

4.6 The step-change of input voltage, reference current of the battery, the reference voltage of battery and current load

In the performed simulation, the initial operation point of the system has been chosen randomly. In this situation, the battery voltage and current, input voltage, and load all change stepwise one second after the start of the simulation simultaneously. In Figurer(c) and (d) of Figure 9, the values 20% higher and lower than the battery voltage and current are displayed in green. As seen in Figure9, within a brief interval, the voltage and current of the battery remain within a range of 20% of their permanent value. The control indicators for this situation are presented in Table 2.
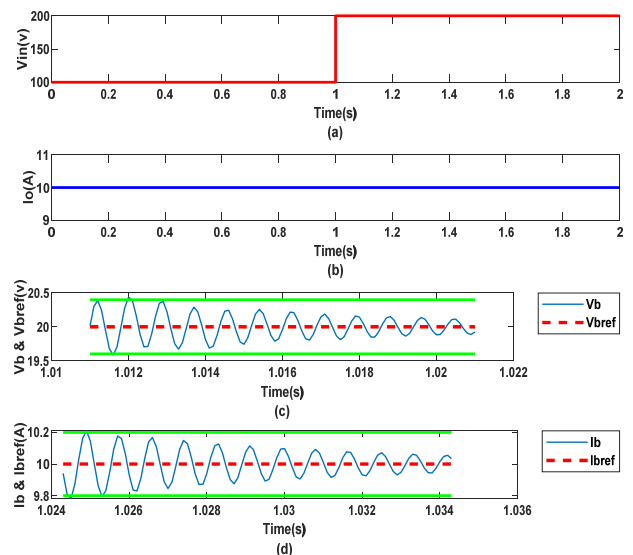

Fig. 4. Simulation result in steady-state condition

4.5 The step-change of current load

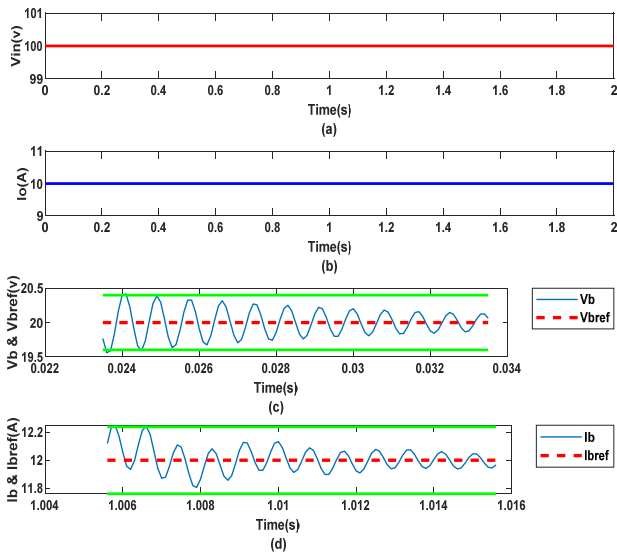**Fig. 5.** Simulation result for step change in input voltage

Fig. 6. Simulation result for step change in reference current of battery
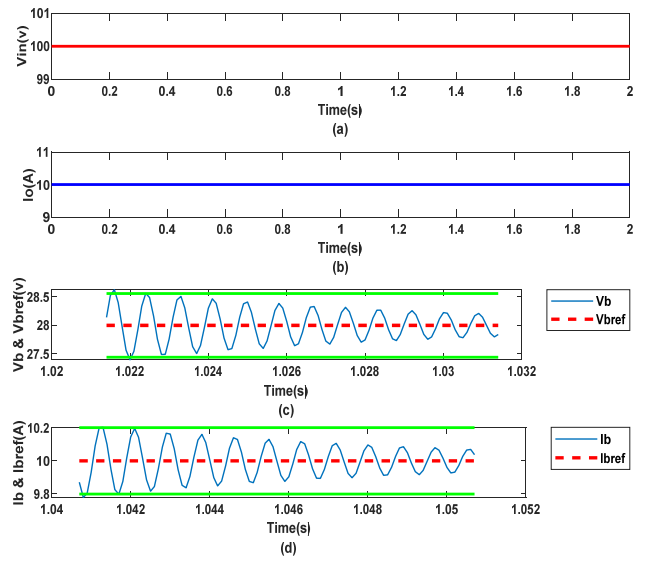

Fig. 7. Simulation result for step change in reference voltage of battery

5. Conclusions

In this study, the effectiveness of placing a battery parallel to the capacitor in a QZSI has been investigated. To control the circuit, a passivity-based controller with interconnection and damping matrix is used to regulate the battery current and voltage. Because this controller is designed based on the large-signal model of the system, it ensures stability over a wide range. Simulations show that the designed controller is robust to changes in different variables, such as input voltage, input current, voltage reference of the battery, and load current. Thus, it is demonstrated that the QZSI with a battery can be easily implemented in renewable energy systems where the voltage of the source fluctuates significantly. In future work, the proposed system can be practically implemented using the introduced control method. Moreover, the effect of parasitic elements must be taken into consideration during the control analysis. To make the system more realistic, a model of renewable systems should replace the input voltage source.
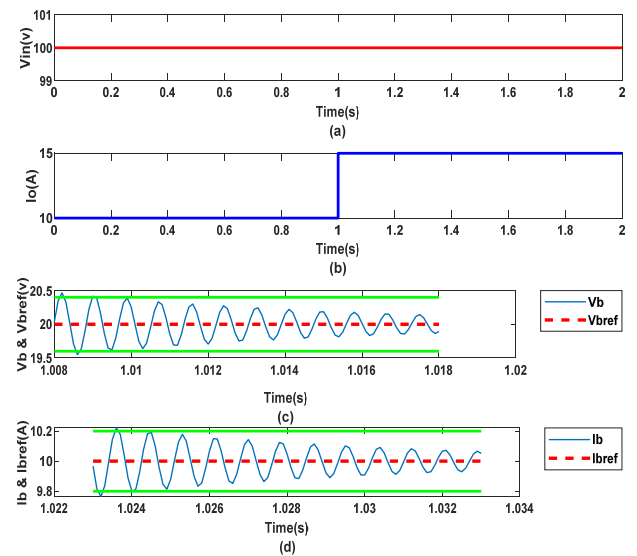

Fig. 8. Simulation result for step change in load current

Table 2. Variations of input voltage, reference current of the battery, reference voltage of the battery and current load

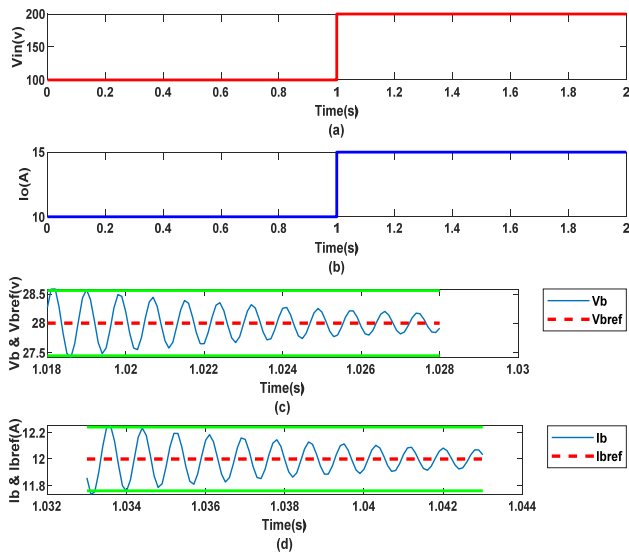| Subnumber of simulation	Vb			Ib		
	Settling-Time	Rise-Time	Steady-state Error	Settling-Time	Rise-Time	Steady-state Error
4-1	20ms	0.3ms	0	30ms	2.2ms	0
4-2	10ms	0.3ms	0	20ms	2.2ms	0
4-3	20ms	0.3ms	0	6.6ms	2.2ms	0
4-4	20ms	0.4ms	0	40ms	2.2ms	0
4-5	9ms	0.3ms	0	20ms	2.2ms	0
4-6	10ms	0.4ms	0	30ms	2.2ms	0

Fig. 9. Simulation result for step change in input voltage, reference current of battery, reference voltage of battery and load current

References

[1] F. Z. Peng, "Z-source inverter," *IEEE Transactions on industry applications,* vol. 39, no. 2, pp. 504-510, 2003.

[2] O. Ellabban and H. Abu-Rub, "Z-source inverter: Topology improvements review," *IEEE Industrial Electronics Magazine,* vol. 10, no. 1, pp. 6-24, 2016.

[3] S. Padmanaban, P. K. Maroti, J. B. Holm-Nielsen, F. Blaabjerg, Z. Leonowicz, and V. Yaramasu, "Quazi Z-source single stage high step-up DC-DC converter for grid-connected PV application," in *2019 IEEE International Conference on Environment and Electrical Engineering and 2019 IEEE Industrial and Commercial Power Systems Europe (EEEIC/I&CPS Europe)*, 2019, pp. 1-6: IEEE.

[4] P. B. Miyani and A. V. Sant, "Lead compensator-based voltage control of quasi Z-source inverter for grid integration of photovoltaic system," *International Journal of Ambient Energy,* vol. 44, no. 1, pp. 46-56, 2023.

[5] E. P. Soares-Ramos, L. De Oliveira-Assís, R. Sarrias-Mena, P. García-Triviño, C. A. García-Vázquez, and L. M. Fernández-Ramírez, "Averaged Dynamic Modeling and Control of a Quasi-Z-Source Inverter for Wind Power Applications," *IEEE Access,* vol. 9, pp. 114348-114358, 2021.

[6] P. Wang, L. Zhou, Y. Zhang, J. Li, and M. Sumner, "Input-parallel output-series DC-DC boost converter with a wide input voltage range, for fuel cell vehicles," *IEEE Transactions on Vehicular Technology,* vol. 66, no. 9, pp. 7771-7781, 2017.

[7] Q. Lei, D. Cao, and F. Z. Peng, "Novel loss and harmonic minimized vector modulation for a current-fed quasi-Z-source inverter in HEV motor drive application," *IEEE Transactions on Power Electronics,* vol. 29, no. 3, pp. 1344-1357, 2013.

[8] T. Na, Q. Zhang, S. Dong, H. J. Raherimihaja, G. Chuai, and J. Wang, "A soft-switched modulation for a single-phase quasi-Z-source-integrated charger in electric vehicle application," *IEEE Transactions on Power Electronics,* vol. 35, no. 5, pp. 4602-4612, 2019.

[9] M. Bharat, A. Murty, and R. Dash, "Design and analysis of trans Z-source inverter for electric vehicle applications using neural network-clustering," *Bulletin of Electrical Engineering and Informatics,* vol. 12, no. 3, pp. 1783-1796, 2023.

[10] S. N. Rao and P. Kumar, "Performance analysis of Z-source inverter topologies for renewable energy sources and fuel cell applications," in *2020 IEEE International Conference on Distributed Computing, VLSI, Electrical Circuits and Robotics (DISCOVER)*, 2020, pp. 165-170: IEEE.

[11] J. Liu, S. Jiang, D. Cao, X. Lu, and F. Z. Peng, "Sliding-mode control of quasi-Z-source inverter with battery for renewable energy system," in *2011 IEEE Energy Conversion Congress and Exposition*, 2011, pp. 3665-3671: IEEE.

[12] U. Shinde, S. Kottagattu, S. Kadwane, and S. Gawande, "Grid-connected quasi-z-source inverter with battery," *Turkish Journal of Electrical Engineering and Computer Sciences,* vol. 26, no. 4, pp. 1847-1859, 2018.

[13] S. Samanta, S. Barman, J. P. Mishra, P. Roy, and B. K. Roy, "Design of an interconnection and damping assignment-passivity based control technique for energy management and damping improvement of a DC microgrid," *IET Generation, Transmission & Distribution,* vol. 14, no. 11, pp. 2082-2091, 2020.

[14] S. Pang *et al.*, "Interconnection and damping assignment passivity-based control applied to on-board DC–DC power converter system supplying constant power load," *IEEE Transactions on Industry Applications,* vol. 55, no. 6, pp. 6476-6485, 2019.